

# Tutorial for the Strength Design of Embedded Rack Railway Structures

**Zoltán Major, Attila Németh, Vivien Jóvér, Dániel Harrach,  
Gusztáv Baranyai and Szabolcs Fischer\***

Széchenyi István University,  
Central Campus Győr; and Vehicle Industry Research Center  
Egyetem tér 1, H-9026 Győr, Hungary  
{majorz,nemeth.attila,jover.vivien,harrda,baranyai.gusztav,fischersz}@sze.hu  
\*Corresponding author

---

*Abstract: Rack railways have made it possible to run trains in steep and mountainous areas, by offering better traction and stability. This paper takes a closer look at the design challenges and practical solutions involved in upgrading these systems – especially when moving from traditional fish-plated jointed tracks to continuously welded rails in embedded track configurations. The authors focused on the forces acting on the rack, how thermal expansion is handled and what happens where tracks meet bridges. Using analytical methods and Finite Element Analysis (FEM), this work examines how different loads and temperatures affect the rack's performance, especially in tight curves and high-gradient areas. The findings highlight the importance of flexible support structures, strong anchorage, and the use of durable rail profiles like TN70. The study also underscores how small design tweaks – like adjusting geometry or material properties – can go a long way in boosting both performance and lifespan. Overall, this work contributes to building safer, longer-lasting rack railway systems, that are easier to maintain over time.*

*Keywords: embedded rack railway; mountain railway; civil engineering; continuously welded rail; finite element analysis*

---

## 1 Introduction

Rail transport is essential to modern society, enabling both passenger and freight movement in towns and cities [1-4]. Among fixed systems, public railways and urban railways (e.g., subways and tramways) are notable. Subways, especially in capital cities, support millions of daily commuters independently from surface traffic, reaching speeds up to 80 km/h. Tramways, typically at ground level, run at 50 km/h, while local interest lines (e.g., Budapest's H lines) operate between 50-80 km/h [5]. Special systems include cableways, funiculars, and rack railways.

Railways are built either with crushed stone ballast or on rigid slab structures [6] [7]. Most substructures use earthworks, though foundation conditions may vary, especially in soft ground [8]. Rails are linked via fish-plated or welded joints [9] [10], fixed to supports by fasteners. Damping vibrations [11] [12] and maintaining structural and geometric stability are critical, supported by flexible materials [13] [14].

Electric rail transport is efficient and eco-friendly [15-17], but track defects – measured using methods like 3D scanning [18] – increase energy usage. Maintaining proper geometry lowers long-term operational costs [15] [16].

This article focuses on the rack railways that are vital in steep terrains. These systems feature a toothed rack alongside tracks to aid traction on inclines [19]. Originating in the 19<sup>th</sup> Century, the first was Switzerland's Rigi Railway (1863), followed by Austria and Germany's systems [19]. Steam-powered rack trains enabled heavier loads, later improved by electric traction in the mid-20<sup>th</sup> Century [20].

Today, rack railways are vital in mountainous areas, used for both tourism and transport in places like Switzerland's Gornergrat Line. Modern materials and design ensure durability [19]. Countries like Japan and New Zealand have adopted the system, with Europe investing in intelligent management and automated maintenance [21].

Challenges remain in sustainability and energy sourcing. Expanding into freight transport is under exploration [22]. Overall, rack railways remain integral for overcoming terrain limitations.

These systems use a gear-to-rack interface to manage steep inclines [23], with efficiency influenced by tooth design [24]. Speed, slope, and dynamic forces affect load distribution, while optimized geometry improves durability [25]. Simulations reveal non-linear force behaviors [26], and FEA aids in reducing stress concentrations [27] [28]. Innovative connections increase failure tolerance [29].

Seismic resilience is vital, supported by advanced materials and real-time sensing [30] [31]. Gear-rack contact wear affects energy efficiency, monitored through inspection regimes [32]. Mountainous operation requires stress distribution modeling under variable loads [24].

Braking and acceleration create dynamic loads that impact structural integrity [33] [34]. Sustainability goals drive the use of eco-friendly materials while retaining performance [35], and innovations in smart materials and simulations aim to boost safety [36].

Frydrysek et al. [37] validated FEA for analyzing stresses in rail anchors on slopes up to 25°. Shen et al. [38] explored gear-rack meshing under track irregularities. Hyeoung-Deok et al. [39] studied precast concrete systems for steep terrains. Zhenhuan et al. [40] examined friction effects in gear-rack and wheel-rail

interactions. Haowen et al. [41] modeled dynamic behavior for smooth gear transitions. Hao et al. [42] addressed longitudinal stability in CWR systems (continuously welded rail tracks) on bridges. Qingjun et al. [43] proposed central anchorage solutions for high-gradient rails. Hyeoung-Deok et al. [44] optimized shear anchor designs for mountain rack rail tracks.

The literature on embedded rack railway structures highlights significant advancements in design, material selection, and performance optimization. Rack railway systems, first introduced in the 19<sup>th</sup> Century, have evolved substantially with improvements in traction mechanisms, load distribution strategies, and track reinforcement techniques. Early research primarily focused on developing gear-rack meshing dynamics and enhancing power transmission efficiency for steep gradients. The introduction of electric propulsion in the mid-20<sup>th</sup> Century significantly increased operational reliability and reduced costs. Recent studies emphasize finite element analysis (FEA) to optimize track strength, material fatigue resistance, and seismic performance, ensuring the durability of railway infrastructure in mountainous terrains. Advances in computational modeling have allowed for real-time monitoring of structural stresses, leading to more adaptive maintenance strategies. The literature also discusses the role of embedded track systems, which enhance stability by providing lateral support in high-gradient sections. Comparative research on international rack railway designs has contributed to standardizing best practices, integrating sustainable materials, and improving overall railway safety. Additionally, ongoing efforts aim to integrate predictive maintenance technologies, such as intelligent train management systems, to further refine performance. Despite these advancements, challenges remain in enhancing track longevity, minimizing wear on gear-rack interfaces, and optimizing structural responses under extreme environmental conditions.

While existing studies extensively cover gear-rack interaction, material enhancements, and dynamic load distribution, there remains a gap in understanding the long-term structural behavior of continuously welded embedded rack railway tracks. Most research focuses on conventional rack systems with jointed rails, while the transition to embedded CWR systems introduces new technical challenges, such as managing expansion forces, mitigating thermal stresses, and optimizing lateral stability. The available literature provides insights into individual components, but holistic models integrating track geometry, material fatigue, and real-world operational factors remain limited. Furthermore, research on the influence of seismic activity on embedded CWR rack railways is still in its early stages, requiring more comprehensive studies that incorporate real-time monitoring techniques. Another critical gap is the need for advanced numerical simulations that combine multi-body dynamics with real-world operational data to refine track design methodologies. Addressing these gaps are essential for ensuring the long-term safety, efficiency, and adaptability of embedded rack railway systems, particularly in high-gradient, high-load environments.

The structure of the current paper is the following: Section 2 deals with the materials and methods and calculation procedures, Section 3 summarizes and concludes the main findings of the article in a structured form.

## 2 Methods and Calculation Procedures

The design of the reconstruction and extension of the Budapest Rack Railway, opened in 1871, is one of the most interesting engineering challenges of our time. The conversion of the currently jointed track (track with fish-plated rail joints) into a continuously welded rail one requires special technical interventions. These include, for example, the lateral/side support of small-span curves or the design of the superstructure.

In the early stages of the design, a number of different track layouts were considered, including an embedded track layout. The new racks will be of the Strub type, as before, but will be made from TN70 rails instead of the DS100 crane rails currently used. The TN70 and DS100 rails are illustrated in Figure 1.

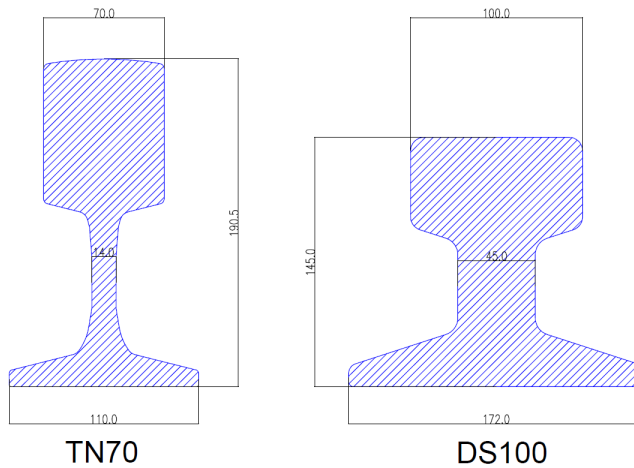


Figure 1

The TN70 and DS100 rail profiles and their geometrical dimensions (dimensions are given in mm)

### 2.1 Determination of the Forces Acting on the Rack Tooth

The first step in calculating the forces acting on the rack [45] is to determine the braking force ( $V$ ) parallel to the axis of the rack tooth path. This can be calculated using the following formulae. The forces acting on the rack tooth and the parametric dimensions of the rack tooth are illustrated in Figure 2.

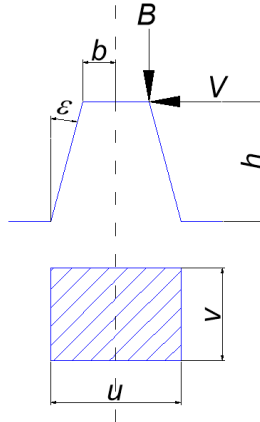


Figure 2

Forces on the rack tooth and its dimensions

The magnitude of the total braking force ( $\Sigma V$ ) is shown in Eq. (1).

$$\Sigma V = (Q_{loc.} + Q_{wag.}) \cdot \left[ 1000 \cdot (1 + \xi) \cdot \frac{a}{g} + \mu_e - \mu \right] \quad (1)$$

where  $Q_{loc.}$  and  $Q_{wag.}$  are the weights of the locomotive and wagons, respectively in kN,  $\xi$  is the weight increasing member,  $a$  is the deceleration of braking in  $\text{m/s}^2$ ,  $g$  is the gravity ( $9.81 \text{ m/s}^2$ ),  $\mu_e$  is the climbing resistance in ‰ (see Figs. 3 and 4).

The magnitude of the braking force acting on a braked rack tooth is calculated according to Eq. (2):

$$V = \frac{\Sigma V}{n} \quad (2)$$

The recommended values for the weight increasing member ( $\xi$ ) are the followings [45]:

- Electric geared cog-wheel wagon/train:  $\xi=0.15\ldots0.24$
- Electric geared cog-wheel locomotive:  $\xi=1.36\ldots1.43$
- Passenger wagon:  $\xi=0.06$
- Cog-wheel train (one locomotive and two passenger wagons):  $\xi=0.53$

The recommended average running resistances ( $\mu$ ) are the followings [45]:

- Wagon with normal gauge, two axles:  $\mu=4$
- Wagon with normal gauge, four axles:  $\mu=3$
- Wagon with 1000mm gauge:  $\mu=3\ldots7$
- Electric geared cog-wheel locomotive with standard track gauge:  $\mu=7\ldots12$
- Electric geared cog-wheel locomotive with 1000mm track gauge:  $\mu=8\ldots10$
- Train-wagon for electric traction:  $\mu=6\ldots10$

The steepness of the inclination of the rack railway path no longer allows the use of the same relations for small angles. In this case, the formula for the climbing resistance to climb takes the following form (see Eq. (3)).

$$\mu_e = e - \Delta e \quad (3)$$

The relationship between the  $e$  and  $\Delta e$  values is illustrated in Fig. 3. The values of  $\mu_e$  are illustrated in Fig. 4.

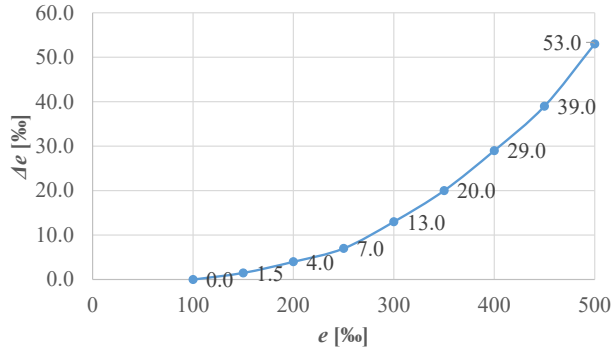


Figure 3

The relationship between  $e$  and  $\Delta e$

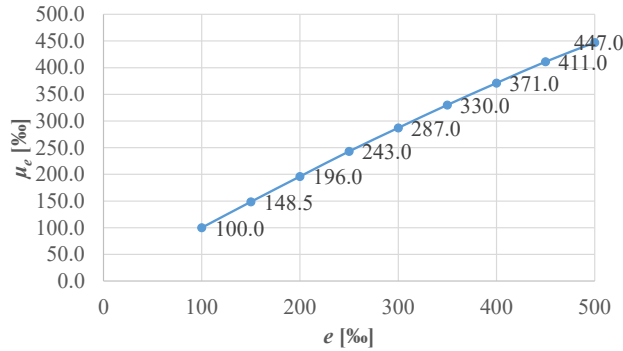


Figure 4

The values of  $\mu_e$

In a second step, the component ( $B$ ) of the acting force perpendicular to the track axis can be determined from Eq. (4) in case of sliding down:

$$B = V \cdot \frac{tg(\epsilon) + f}{1 - f \cdot tg(\epsilon)} \quad (4)$$

In the case of climbing uphill, Eq. (5) can be applied:

$$B = V \cdot \frac{\operatorname{tg}(\varepsilon) - f}{1 + f \cdot \operatorname{tg}(\varepsilon)} \quad (5)$$

The value of  $f$  depends on the roughness of the surfaces. Its magnitude varies between 0.25 and 0.05. The value of  $\operatorname{tg}(\varepsilon)$  in Hungarian practice is usually 0.25.

The formula presented for calculating the value of  $B$  can be rewritten by introducing the quantity  $C$ . The relationship between the value of  $C$  and the value of  $f$  is illustrated in Fig. 5 for  $\operatorname{tg}(\varepsilon)=0.25$  according to Eq. (4) and Fig. 6 as in Eq. (5).

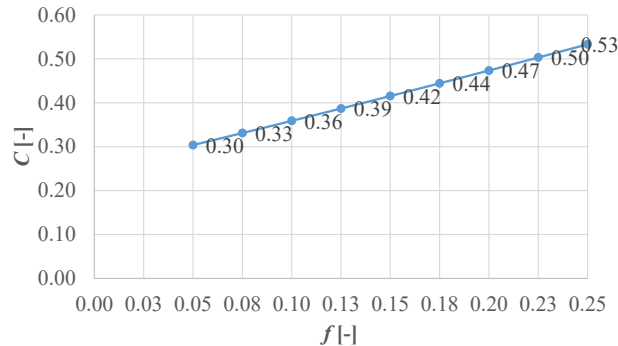


Figure 5

The values of  $C$  according Eq. (4)

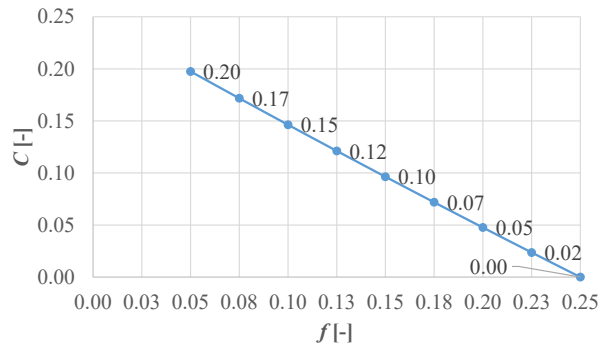


Figure 6

The values of  $C$  according to Eq. (5)

## 2.2 Checking the Strength of the Rack

The dimensioning of rack and pinion of the webbing design was previously done as a rigidly double-supported structure. The supporting system was designed to be bended only in the vertical plane moment caused by forces  $B$  and  $V$ . In the present case, however, neither the thermal force nor the normal force due to the  $V$  force can be ignored in the continuously welded (CW) rack. A test of the support for

horizontal plane bending is also presented. The current analysis is presented for effects caused by a single gear. The effect of multiple gears can be determined by linear superposition. The strength properties of the rack can be easily determined using AxisVM software with the knowledge of the post-machining geometry.

### 2.3 Calculation of the Normal Forces in the Rack

Thanks to the CW design and the flexible embedding, the rack experiences normal force even under  $V$  force and temperature variations. This are illustrated in Figs. 7-8 and Eqs. (6-9).

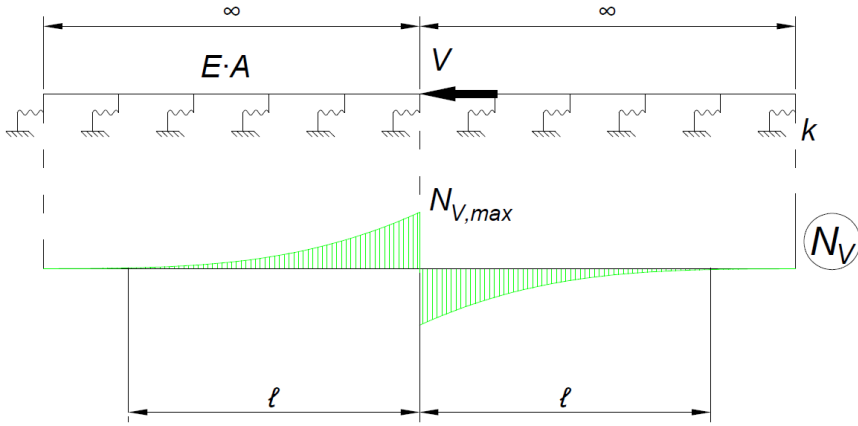


Figure 7  
Normal force from the  $V$  force

$$N(x) = \frac{V}{2} \cdot f_1(x) \quad (6)$$

$$f_1(x) = e^{-\sqrt{\frac{k}{EA}}x} \quad (7)$$

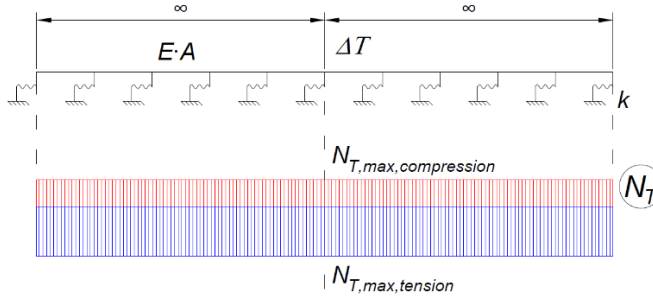


Figure 8  
Normal force from the temperature variations



$$N(x)_{T,compression} = E \cdot \alpha \cdot A \cdot \Delta T_{compression} = const. \quad (8)$$

$$N(x)_{T,tension} = E \cdot \alpha \cdot A \cdot \Delta T_{tension} = const. \quad (9)$$

## 2.4 Calculation of the Bending Moments in the Rack

Three effects generate bending moments in the rack. Vertical plane bending is due to the externality ( $y$ ) of force  $V$  and on the impact of force  $B$  (see Fig. 9 and Eqs. (10-15)). In the horizontal plane, the bending moment is also due to the externality ( $e$ ) of force  $V$  (see Fig. 10 and Eqs. (16-19)). It is this inaccuracy/externality that causes the torsional effect when dimensioning the rack tooth.

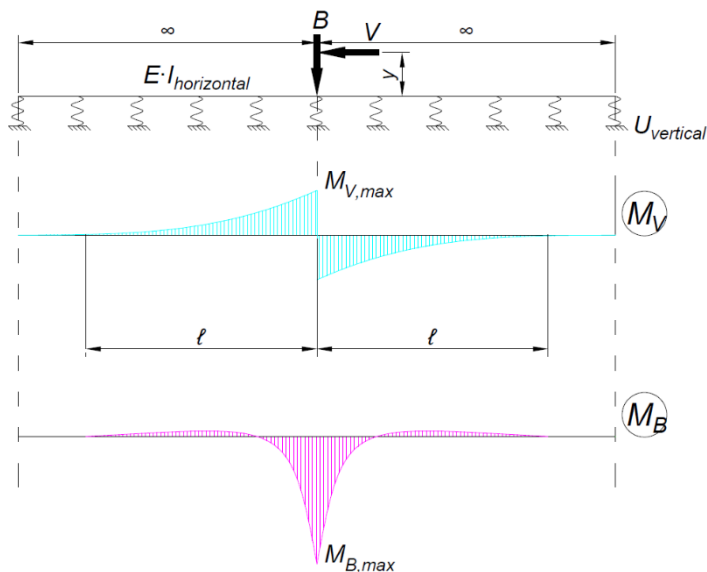


Figure 9

Vertical plane bending moment developed in the rack

$$M_V(x) = \frac{V \cdot y}{2} \cdot f_2(x) \quad (10)$$

$$M_B(x) = \frac{B \cdot L_f}{4} \cdot f_3(x) \quad (11)$$

$$L_f = \sqrt[4]{\frac{4 \cdot E I_{horizontal}}{U_{vertical}}} \quad (12)$$

$$\xi_f = \frac{x}{L_f} \quad (13)$$

$$f_2(x) = e^{-\xi_f} \cdot \cos(\xi_f) \quad (14)$$

$$f_3(x) = e^{-\xi_f} \cdot (\cos(\xi_f) - \sin(\xi_f)) \quad (15)$$

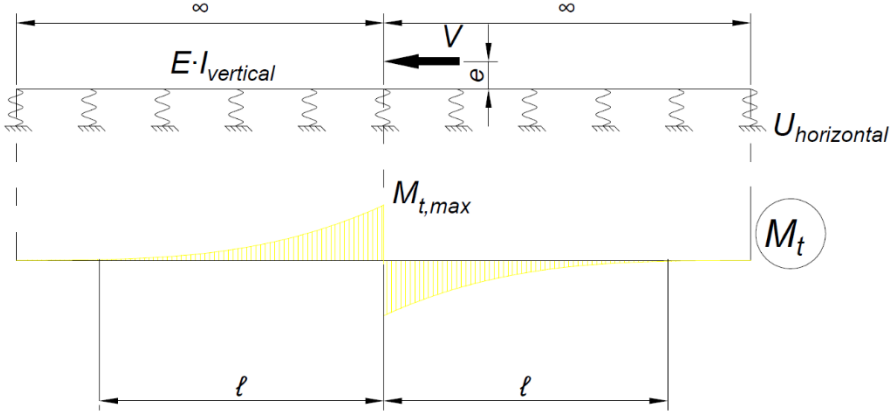


Figure 10  
Horizontal plane bending moment developed in the rack

$$M_t(x) = \frac{V \cdot e}{2} \cdot f_4(x) \quad (16)$$

$$L_v = \sqrt[4]{\frac{4 \cdot E I_{vertical}}{U_{horizontal}}} \quad (17)$$

$$\xi_v = \frac{x}{L_v} \quad (18)$$

$$f_4(x) = e^{-\xi_v} \cdot \cos(\xi_v) \quad (19)$$

## 2.5 Additional Stress Evolving in the Rack

On bridges where the rack and rail pass without a gap, over the discontinuities in the supporting structure, the bridge structure and the track together, take up the starting and braking forces. One part of these is transferred to the backfill and another part to the foundation through the substructure.

If the CW rack and rail prevents displacements of the superstructure, longitudinal forces will occur in the rails and fixed supports of the bridge. These effects are called the track-bridge interaction and must be taken into account in the calculation of the superstructure, support bearings and substructure(s), and in the determination of the stresses on the rack, rail and rail fastenings. The effects in the rack are

calculated by finite element modelling and can be summed with the previously calculated effects using linear superposition.

## Conclusions

This study provides practical insights into the design and performance of embedded rack railway systems, particularly during the transition from traditional jointed rails to continuously welded rail (CWR) configurations. While the shift offers clear advantages – such as improved ride quality, reduced maintenance, and enhanced long-term stability – it also introduces new engineering challenges that must be addressed with care.

Thermal expansion emerged as a critical factor. Unlike jointed tracks, continuously welded systems lack natural expansion gaps, causing thermal stresses to accumulate within the structure. Through analytical methods and simulation, the behavior of these forces was evaluated, and design strategies such as flexible supports, suitable materials, and controlled load transfer paths were identified as effective solutions.

The geometry of the rack system was also found to significantly influence stress distribution, especially at gear-rack interfaces on steep gradients or tight curves. The use of TN70 rail profiles, offering better mechanical properties than the previously used DS100 sections, was shown to reduce localized stresses and improve durability.

Track-bridge interaction was highlighted as another key consideration. Since longitudinal forces caused by braking and acceleration are transmitted through the rail into the bridge, it is essential for the rail and supporting structure to be designed as an integrated system. Addressing this interaction during the early design stages contributes to overall structural safety and resilience.

In conclusion, embedded rack railways with continuously welded rails represent a modern, high-performance solution for rail transport in steep and challenging environments. However, successful implementation depends on detailed analysis, systems-based design, and the continued development of predictive tools and resilient materials to ensure long-term reliability and sustainability.

## Nomenclature:

- $\Sigma V$  total braking force [kN]
- $a$  the deceleration of braking [ $\text{m/s}^2$ ]
- $A$  the machined cross-sectional area of the rack [ $\text{m}^2$ ]
- $B$  vertical force acting on the rack [kN]
- $C$  auxiliary quantity [-]
- $e$  distance between the force  $V$  and the center of gravity of the roughed/machined rack in the horizontal plane [m] ( $e=0.025$  m)
- $E$  elastic modulus of the rack [ $\text{kN/m}^2$ ]
- $f$  the coefficient of creep-friction [-]

$I_{horizontal}$	is the inertia of the roughed/machined rack with respect to the horizontal axis [m <sup>4</sup> ]
$I_{vertical}$	is the inertia of the machined/roughed rack on the vertical axis [m <sup>4</sup> ]
$k$	longitudinal spring constant/rate [kN/m/m]
$n$	the number of braked gears [piece]
$Q_k$	the weight of the wagons [kN]
$Q_{loc.}$	weight of the locomotive [kN]
$Q_m$	weight of the locomotive [kN]
$Q_{wag.}$	total weight of the wagons [kN]
$U_{horizontal}$	elasticity factor/coefficient of lateral support of the rack [kN/m/m]
$U_{vertical}$	elasticity coefficient/factor of the rack support [kN/m/m]
$V$	braking force [kN]
$x$	distance from force $V$ [m]
$y$	the distance between the force $V$ and the center of gravity of the machined/roughed rack [m]
$\alpha$	linear coefficient of thermal expansion of the rack [1/°C]
$\Delta T_{compression}$	difference between +60 °C and the neutral temperature [°C]
$\Delta T_{tension}$	the difference between –30 °C and the neutral temperature [°C]
$\varepsilon$	angle of the rack tooth jacket [°]
$\mu$	the value of the average running resistance [N/kN]
$\mu_e$	the climbing resistance [%]
$\zeta$	the mass increasing member [-]

## Acknowledgement

This paper was prepared by the research team "SZE-RAIL". This research was supported by SIU Foundation's project 'Sustainable railways – Investigation of the energy efficiency of electric rail vehicles and their infrastructure'. The publishing of the paper did not receive financial support or financing of the APC.

## References

- [1] J. Holzfeind, J. Liu, F. Pospischil (Eds.). Railroad infrastructure handbook, 4th edition (original title in German: Handbuch Eisenbahninfrastruktur). Springer Vieweg, Berlin, Heidelberg, Germany, 2024 (in German)
- [2] I. Taran, A. Karsybayeva, V. Naumov, K. Murzabekova, M. Chazhabayeva. Fuzzy-Logic Approach to Estimating the Fleet Efficiency of a Road Transport Company: A Case Study of Agricultural Products Deliveries in Kazakhstan. Sustainability, Vol. 15(5), 2023, 4179
- [3] M. Oleskevych, I. Taran, T. Volkova, I. Klymenko. Simulation of cargo delivery by road carrier: case study of the transportation company. Naukovyi

- Visnyk Natsionalnoho Hirnychoho Universytetu, Vol. 2022(2), 2022, pp. 118-123
- [4] O. Novytskyi, I. Taran, Z. Zhanbirov. Increasing mine train mass by means of improved efficiency of service braking. E3S Web of Conferences, Vol. 123, 2019, 01034
- [5] V. Jóvér, Z. Major, A. Németh, M. Sysyn, D. Kurhan, S. Fischer. Investigation of the geometrical deterioration process of tramway superstructure systems – A case study. Acta Polytechnica Hungarica, Paper 7157, 2025 (accepted manuscript)
- [6] L. Ézsiás, R. Tompa, S. Fischer. Investigation of the possible correlations between specific characteristics of crushed stone aggregates. Spectrum of Mechanical Engineering and Operational Research, Vol. 1(1), 2024, pp. 10-26
- [7] S. Fischer. Investigation of the Settlement Behavior of Ballasted Railway Tracks Due to Dynamic Loading. Spectrum of Mechanical Engineering and Operational Research, Vol. 2(1), 2025, pp. 24-46
- [8] U. Gerber, M. Sysyn, J. Zarour, O. Nabochenko. Stiffness and strength of structural layers from cohesionless material. Archives of Transport, Vol. 49(1), 2019, pp. 59-68
- [9] S. Fischer, D. Harangozó, D. Németh, B. Kocsis, M. Sysyn, D. Kurhan, A. Brautigam. Investigation of heat-affected zones of thermite rail welding. Facta Universitatis, Series: Mechanical Engineering, Vol. 22(4), 2024, pp. 689-710
- [10] A. Németh, S. Fischer. Investigation of the glued insulated rail joints applied to CWR tracks. Facta Universitatis, Series: Mechanical Engineering, Vol. 19(4), 2021, pp. 681-704
- [11] J. Dižo, M. Blatnický, J. Harušinec, A. Suchánek. Assessment of dynamics of a rail vehicle in terms of running properties while moving on a real track model. Symmetry, Vol. 14(3), 2022, pp. 536
- [12] E. Mikhailov, S. Semenov, H. Shvornikova, J. Gerlici, M. Kovtanets, J. Dižo, M. Blatnický, J. Harušinec. A study of improving running safety of a railway wagon with an independently rotating wheel's flange. Symmetry, Vol. 13(10), 2021, pp. 1955
- [13] A. J. T. Kuchak, D. Marinkovic, M. Zehn. Parametric investigation of a rail damper design based on a lab-scaled model. Journal of Vibration Engineering & Technologies, Vol. 9(1), 2021, pp. 51-60
- [14] A. J. T. Kuchak, D. Marinkovic, M. Zehn. Finite element model updating – Case study of a rail damper. Structural Engineering and Mechanics, Vol. 73(1), 2020, pp. 27-35

- [15] S. Fischer, B. Hermán, M. Sysyn, D. Kurhan, S. Kocsis Szürke. Quantitative analysis and optimization of energy efficiency in electric multiple units. *Facta Universitatis, Series: Mechanical Engineering*, Paper 13299, 2025 (accepted manuscript), <https://doi.org/10.22190/FUME241103001F>
- [16] S. Fischer, S. K. Szürke. Detection process of energy loss in electric railway vehicles. *Facta Universitatis, Series: Mechanical Engineering*, Vol. 21(1), 2023, pp. 81-99
- [17] S. Kocsis Szürke, G. Kovács, M. Sysyn, J. Liu, S. Fischer. Numerical Optimization of Battery Heat Management of Electric Vehicles. *Journal of Applied and Computational Mechanics*, Vol. 9(4), 2023, pp. 1076-1092
- [18] S. Szalai, B. F. Szívós, D. Kocsis, M. Sysyn, J. Liu, S. Fischer. The Application of DIC in Criminology Analysis Procedures to Measure Skin Deformation. *Journal of Applied and Computational Mechanics*, Vol. 10(4), 2024, pp. 817-829
- [19] L. Shen, Z. Zhou, X. Wu, S. He, N. Yang, Y. Luo. Study on the gear-rack meshing dynamic performance based on a multi-body dynamic model of rack rail vehicle. *Advances in Mechanical Engineering*, Vol. 16(9), 2024, 16878132241286640
- [20] H. Lee, S. Han, J. Lim, K. Eum, S. Kim, Y. Kang. Evaluation of structural stresses of mountain-embedded railway systems. *Applied Sciences*, Vol. 13(20), 2023, 11469
- [21] M. Steuer, M. Krzykowski, D. Simiński, W. Chema, R. Burdzik. Train detection methods as the foundation of positioning systems of railroad traffic control. *Diagnostyka*, Vol. 24(3), 2023, pp. 1-7
- [22] A. Dolinayová, V. Zitrický, L. Černá. Decision-making process in the case of insufficient rail capacity. *Sustainability*, Vol. 12(12), 2020, 5023
- [23] K. Nagao, K. Okubo, T. Fujii, S. Uchida. Reduction of maximum torque of driving shafts concurrently driven by rubber v-belt for monorail traveling on worn rack rail for construction uses. *International Journal of Materials, Mechanics and Manufacturing*, Vol. 5(3), 2017, pp. 196-199
- [24] L. Shen, Z. Zhou, X. Wu, S. He, N. Yang, Y. Luo. Study on the gear-rack meshing dynamic performance based on a multi-body dynamic model of rack rail vehicle. *Advances in Mechanical Engineering*, Vol. 16(9), 2024, 16878132241286640
- [25] Y. Liu, T. Hong, Z. Li. Influence of toothed rail parameters on impact vibration meshing of mountainous self-propelled electric monorail transporter. *Sensors*, Vol. 20(20), 2020, 5880
- [26] M. Gao, P. Wang, Y. Cao, R. Chen, C. Liu. A rail-borne piezoelectric transducer for energy harvesting of railway vibration. *Journal of Vibroengineering*, Vol. 18(7), 2016, pp. 4647-4663

- [27] H. P. Lee, S. Han, J. Lim, K. Eum, S. Kim, Y. J. Kang. Evaluation of structural stresses of mountain-embedded railway systems. *Applied Sciences*, Vol. 13(20), 2023, 11469
- [28] X. Lin, J. R. Edwards, M. S. Dersch, T. A. Roadcap, C. Ruppert. Load quantification of the wheel–rail interface of rail vehicles for the infrastructure of light rail, heavy rail, and commuter rail transit. *Proceedings of the Institution of Mechanical Engineers, Part F: Journal of Rail and Rapid Transit*, Vol. 232(2), 2017, pp. 596-605
- [29] M. Blatnický, J. Dižo, M. Blatnická. Strength reanalysis and influence line equation of rack system drive force. *MATEC Web of Conferences*, Vol. 254, 2019, 02005
- [30] A. Kanyilmaz, G. Brambilla, G. P. Chiarelli, C. A. Castiglioni. Assessment of the seismic behaviour of braced steel storage racking systems by means of full scale push over tests. *Thin-Walled Structures*, Vol. 107, 2016, pp. 138-155
- [31] L. D. Sarno, G. Karagiannakis. Petrochemical steel pipe rack: critical assessment of existing design code provisions and a case study. *International Journal of Steel Structures*, Vol. 20(1), 2019, pp. 232-246
- [32] L. He, Z. Ye. Research on the performance of carbon fiber composite railings for ships. *Academic Journal of Science and Technology*, Vol. 13(2), 2024, pp. 158-164
- [33] W. Salman, C. Fan, H. Pan, Z. Zhang, X. Wu, M. Abdelrahman, A. M. Tairab, A. Ali. A dual-kinetic energy harvester operating on the track and wheel of rail deceleration system for self-powered sensors. *Smart Materials and Structures*, Vol. 32(12), 2023, 125023
- [34] P. Sideris, A. Filiatrault, M. Leclerc, R. Tremblay. Experimental investigation on the seismic behavior of palletized merchandise in steel storage racks. *Earthquake Spectra*, Vol. 26(1), 2010, pp. 209-233
- [35] C. Wang, P. Gao, X. Wang, H. Wang, X. Liu, H. Zheng. Mechanical design and experiments of a new rotational variable stiffness actuator for hybrid passive–active stiffness regulation. *Actuators*, Vol. 12(12), 2023, 450
- [36] G. Vatulia, A. Lovska, Y. Krasnokutskyi. Research into the transverse loading of the container with sandwich-panel walls when transported by rail. *IOP Conference Series: Earth and Environmental Science*, Vol. 1254(1), 2023, 012140
- [37] K. Frydryšek, J. Freis, V. Kolář. Way of stress and deformation calculations in the rails and anchor pins of mining rack-railway track. *Strojnícky časopis – Journal of Mechanical Engineering*, Vol. 74(3), 2024, pp. 27-44
- [38] L. Shen, Z. Zhou, X. Wu, S. He, N. Yang, Y. Luo. Study on the gear-rack meshing dynamic performance based on a multi-body dynamic model of rack

- rail vehicle. *Advances in Mechanical Engineering*, Vol. 16(9), 2024, 16878132241286640
- [39] H. D. Lee, J. K. Song, T. S. Yun, S. Kim, J. Moon. Shear anchor behavior and design of an embedded concrete rack rail track for mountain trains. *Computers and Concrete*, Vol. 33(4), 2024, pp. 373-384
- [40] W. Zhenhuan, Z. Xin, F. Wei, J. Dianxiang, Y. Jizhong, L. Shulin, W. Zhefeng. Analysis of the coupling mechanism between gear-rack meshing and wheel-rail rolling contact of rack railway. *Yingyong Lixue Xuebao/Chinese Journal of Applied Mechanics*, Vol. 41(1), 2024, pp. 58-67
- [41] H. Wang, Q. Xiang, W. Liu, C. Gao, J. Liu, S. Wang, X. Deng. Dynamics Characteristics Analysis of Rack Railway Guiding Equipment of Mountain Rack Railway Train with Considering Wheel-Rail Contact. *ICMD: International Conference on Mechanical Design*, 2023, pp. 2193-2209
- [42] X. Hao, X. Kaize, D. Junqiao, C. Wenfeng, Y. Wenmao, H. Lianjun. Research on the Influence of Seamless Rack on the Continuous Welded Rail on the Simply Supported Girder Bridge. *Journal of Railway Engineering Society*, Vol. 40(6), 2023, pp. 39-45
- [43] L. Qingjun, G. Jinfa, C. Zhan. Scheme and Feasibility Study of Central Anchor with Stay Wire for Contact Rail of Rack Railways. *Railway Standard Design*, Vol. 66(7), 2022, pp. 145-149
- [44] L. Hyeoung-Deok, S. Jong-Keol, M. Jiho. Shear Anchor Behavior and Design of Embedded Rack Rail Track Panel for Mountain Train. *Journal of the Korean Society for Railway*, Vol. 24(11), 2021, pp. 951-962
- [45] A. Horváth, E. Kerkápoly, J. Megyeri. Special railways (original title in Hungarian: “Különleges vasutak”). *Műszaki Könyvkiadó*, Budapest, 1978 (in Hungarian)